Journal of Sound and Vibration (1999) **224**(4), 689–707
Article No. jsvi.1999.2186, available online at http://www.idealibrary.com on IDEAL®

STANDING WAVES IN A RECTANGULAR SOUND BOX RECORDED BY TV HOLOGRAPHY

A. Runnemalm

Division of Experimental Mechanics, Luleå University of Technology, SE-971 87 Luleå, Sweden

(*Received* 15 *June* 1998, *and in final form* 27 *January* 1999)

A simple but informative whole-field method to visualize standing waves in air enclosures is presented. The integrated sound pressure field distribution of standing-wave patterns inside a rectangular, air-filled transparent box is measured using ordinary TV holography (also called ESPI or DSPI). The phase distribution of the sound pressure is measured by using the more complicated, phase-modulated TV holography technique. Standing waves in the box are excited by a loudspeaker. The structural vibration amplitude distribution of the walls of the same box (operational deflection shapes, ODSs) are measured at the same frequencies as the standing waves with the same optical technique. The pressure maps obtained and the corresponding structural ODSs are of great pedagogical value and can be used to verify numerical models, etc. Standing-wave patterns in non-rectangular enclosures, as the sound box of a guitar, illustrates the usefulness of the method.

1. INTRODUCTION

In several textbooks on physics as well as on acoustics, waves in a rectangular box or particles in a box are used as a theoretical model for different phenomena. The description of a rectangular box in a Cartesian co-ordinate system makes the mathematics simple; closed analytical solutions are found. Still today, there are not many experimental methods available which visualize these standing-wave patterns. Lord Rayleigh described for instance standing-wave phenomena in air in his book *Theory of Sound* [1]. He also described experiments in this book. "*The experimental investigation of aerial waves within pipes has been effected with considerable success by Kundt*. [*Pogg. Ann. cxxxv*, 337, 1868]. *To generate waves* (*in a tube*) *is easy enough*; *but it is not easy to invent a method by which they can be effectually examined. Kundt discovered that the nodes of stationary waves can be made evident by dust. A little fine sand or lycopodium seed*, *shaken over the interior of a glass tube containing a vibrating column of air disposes itself in recurring patterns*, *by means of which it is easy to determine the positions of the nodes and to measure the intervals between them*". Kundt's experiment is still used in many secondary physics

0022-460X/99/290689 + 19 $30.00/0

courses to illustrate standing-wave patterns in a non-visible fluid-like medium, as in air. Chladni's figures was a similar method at that time already used to visualize nodal lines of vibration modes of solid objects as membranes, plates and shells [2].

Not many true field measuring methods other than Kundt's experiment are available today by which waves in air can be studied. Of course, there are scanning methods, for instance with a microphone as "point" sensor [3], but, as will be seen below, microphones are quite large and may disturb the sound field. In 1965, hologram interferometry, an interferometric technique, was presented [4], by which it is possible to "see the sound" [5–8]. The reason for this is that a change in sound pressure will also change the air density and the index of refraction. The optical path, which is the product of the index of refraction and the geometrical path length, will be changed for a probing light beam passing through a sound field. This altered optical path of the probing light gives rise to an optical phase shift compared to a light beam passing through an undisturbed air volume. Holographic interferometry is a suitable method to detect such small phase differences. Pulsed holographic interferometry and lately a similar, all electronic technique called pulsed TV holography have been used to detect propagating transient sound fields from impacted plates [5, 6]. Phase-modulated TV holography made it possible to present pictures of propagating harmonic sound fields, "Sound in flight" [7, 8]. Computer tomographic (CT) techniques combined with the measuring methods made it possible to make a full three-dimensional evaluation of propagating sound fields [9–11].

It is however somewhat surprising that standing-wave patterns in air do not seem to have been recorded by using the TV holographic or DSPI methods. The technique to do so is even simpler than the one used to record propagating harmonic sound waves or transients in air. Spatial amplitude maps of the sound pressure fields are easily obtained as will be shown below.

This paper deals with standing waves in air. Both the amplitude and phase are presented for standing waves inside a transparent rectangular box. The box is made of 5 mm thick polymethyl methacrylate (PMMA) and has the dimensions (0·5, 0·3, 0·1) m; see Figure 1. The intergrated sound pressure field inside the box and the structural vibration of the box, are recorded by using ordinary TV holography. To record the phase of the sound pressure field, phase-modulated TV holography is used. One application of this technique might be purely pedagogical. It can be used at universities and laboratories to visualize standing waves and to illustrate such phenomena in textbooks. It is also very useful to illustrate non-simple vibration shapes, as combination modes, as will be shown. The technique can also be used to explore standing-wave patterns in enclosures of any shape like cabins of cars, boats, etc., but also in sound boxes of musical instruments as will be shown. Both the vibrations of the walls of the air enclosure and the standing-wave pattern inside the enclosure can be studied with the same real-time optical TV holography technique. Thus, physical and numerical models of the interaction between the air and the structure can be tested as well as new ideas to decrease or increase the sound pressure fields of the model.

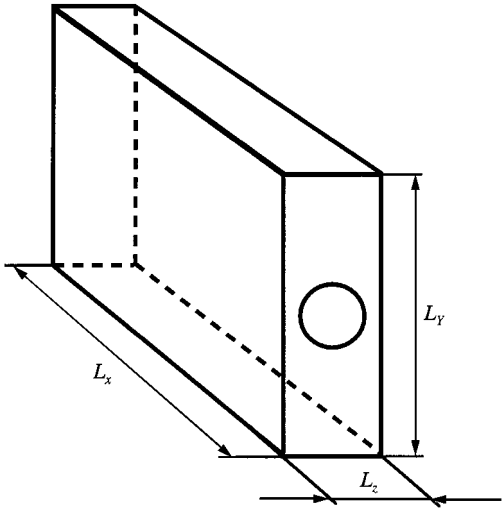

Figure 1. The transparent box is made of 5 mm thick PMMA. The dimension of the box is $(L_x, L_y, L_z) = (0{\cdot}5, 0{\cdot}3, 0{\cdot}1)$ m. In one of the short sides, there is a hole for the loudspeaker.

2. STANDING WAVES IN A BOX

The theory for standing waves in a rectangular box is well described in many text books, for instance in references [12, 13]. Here is a short presentation of the theory.

The sound pressure field $p(x, y, z)$ is described by the Helmholtz equation

$$\nabla^2 p(x, y, z) + k^2 p(x, y, z) = 0, \tag{1}$$

where the operator ∇^2 is the Laplacian operator in Cartesian co-ordinates and k is the wavenumber, equal to ω/c (ω is the angular frequency and c is the speed of sound).

A separable solution of equation (1) is given by

$$p(x, y, z, q) = \Psi(x, y, z, q)\mathrm{e}^{-\mathrm{i}\omega_q t}, \tag{2}$$

where $q = 1, 2, 3, \ldots$. The eigenfunction $\Psi(x, y, z, q)$ must satisfy the boundary conditions for a closed box with rigid walls. It can be shown that the eigenvalue, in equation (1), $k(q)$, in a rectangular cavity can be rewritten as $k_x^2 + k_y^2 + k_z^2 = k^2$ where k_x, k_y and k_z are separable eigenvalues in the three directions. Each eigenvalue has to satisfy the boundary conditions. For a rectangular box with dimensions L_x, L_y and L_z (see Figure 1), this gives $k_x = \pi q_x/L_x$, and so on for k_y and k_z. The eigenmodes will be labelled (q_x, q_y, q_z): i.e., giving the number q of nodal lines in the x, y and z directions.

Since $k(q) = \omega_q/c = 2\pi f_q/c$, where f_q is the qth eigenfrequency, one has

$$f_q = \frac{c}{2}\sqrt{\left(\frac{q_x}{L_x}\right)^2 + \left(\frac{q_y}{L_y}\right)^2 + \left(\frac{q_z}{L_z}\right)^2}. \tag{3}$$

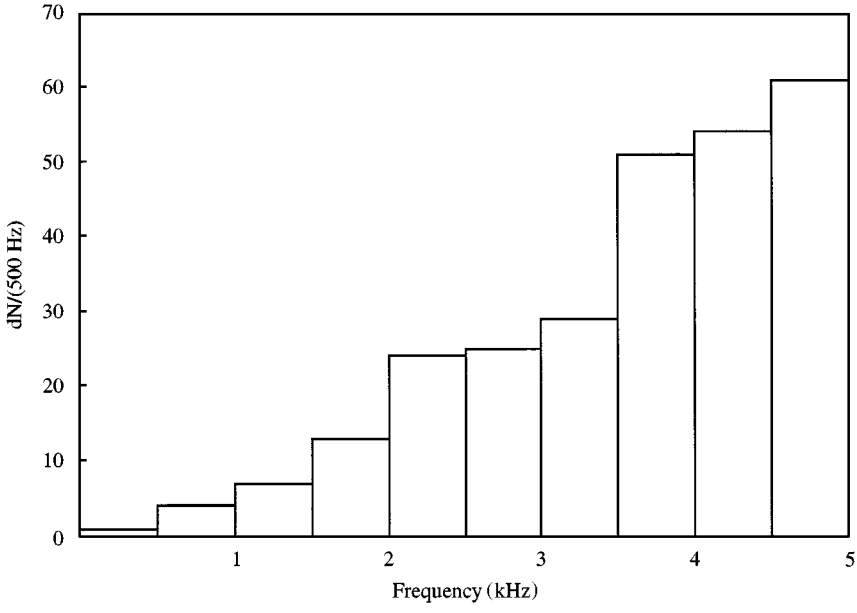

Figure 2. Resonance density for each 500 Hz interval in the rectangular box in Figure 1.

The frequency of a standing wave in the rectangular box depends only upon the speed of sound, c, and the geometrical dimensions (L_x, L_y, L_z) of the box. The number of modes in the box in a frequency interval, increases fast with increasing frequency. The resonance density, i.e., the number of modes within a number of 500 Hz intervals, for eigenmodes (standing waves) is shown in Figure 2. One can see that for increasing frequency the resonance density increases almost exponentially. Therefore combination modes, consisting of several eigenmodes, close in frequency, become more common for increasing frequencies.

3. CHANGE IN OPTICAL PATH BY A SOUND FIELD

A sound pressure gives rise to a change in air density in the sounding medium. The refractive index, n, and the density, ρ, are related through the Gladestone–Dale equation [14]

$$\frac{n-1}{\rho} = \text{constant}. \tag{4}$$

The pressure, p, and the density, ρ, are related through the adiabatic condition,

$$p/p_0 = (\rho/\rho_0)^{\gamma}, \tag{5}$$

where $\gamma = C_p/C_v$ is the adiabatic constant defined by the heat capacities at constant pressure C_p and constant volume C_v. The index 0 refers to the conditions at undisturbed air pressure. Combinating equations (4) and (5) yields a

relation between the change in refractive index due to the sound pressure, $p(x, y, z)$:

$$\Delta n = n(x, y, z) - n_0 = (n_0 - 1)\left[\left(\frac{p(x, y, z)}{p_0}\right)^{1/\gamma} - 1\right]. \tag{6}$$

The optical path difference, Δd, is given by the geometrical path length times the change in refractive index. If it is assumed that the probing ray is travelling along the z-axis and the refractive index is a function of position, the relation between the optical path variation, Δd, and the change in refractive index, $\Delta n = n - n_0$, is

$$\Delta d = \int [n(x, y, z) - n_0]\, \mathrm{d}z. \tag{7}$$

If the refractive index is constant with respect to the integration co-ordinate z and the depth of the sound field is L_z, the optical path difference will simply be the product $\Delta d = L_z \Delta n$. If Δd is measured, Δn can easily be calculated and inserted into equation (6) to extract the actual integrated sound pressure $p(x, y)$ in the box.

If $n(x, y, z)$ varies along the path, several projections are needed to extract the spatial variation (tomography) [9, 10].

4. TV HOLOGRAPHY

TV holography [15–17], sometimes referred to as Electronic Holography, Electro-Optic Holography, Electronic Speckle Pattern Interferometry (ESPI) or Digital Speckle Pattern Interferometry (DSPI), is a real-time non-contract and full-field measuring technique. The measuring principle is based on phase-stepped holographic interferometry. In Figure 3 the optical unit is presented. The transparent sound box is illuminated (see Figure 4) by a frequency-doubled Nd : YAG-laser (wavelength 532 mm). The image field of the box interferes with a smooth reference beam from an optical fibre onto a CCD-detector. The piezo-electric mounted mirror (PZM1) introduces optical phase steps of 90° between subsequent TV frames. The four latest frames are processed on-line by the system. The piezo-electric-mounted mirror PZM2 is used in phase-modulated TV holography; see below. The measurements are presented as high-quality interferograms on a TV monitor in "real time".

With TV holography, vibration analysis of sinusoidally vibrating objects is easily performed. The object is excited by an external exciter at single frequencies. The frequency is changed until an eigenfrequency is found. This occurs when the maximum number of interference fringes appears in the interferogram.

An interferogram of a plate, clamped along the upper and lower edges, vibrating in one of its eigenmode with three antinodes, is shown in Figure 5. Each dark fringe connects points with equal amplitude of vibration and can be interpreted as contour lines on a map. The two white vertical lines are nodal lines with zero vibration amplitude. If the illumination and the object beam are parallel and along the normal of the plate, the intensity distribution on the interferogram is

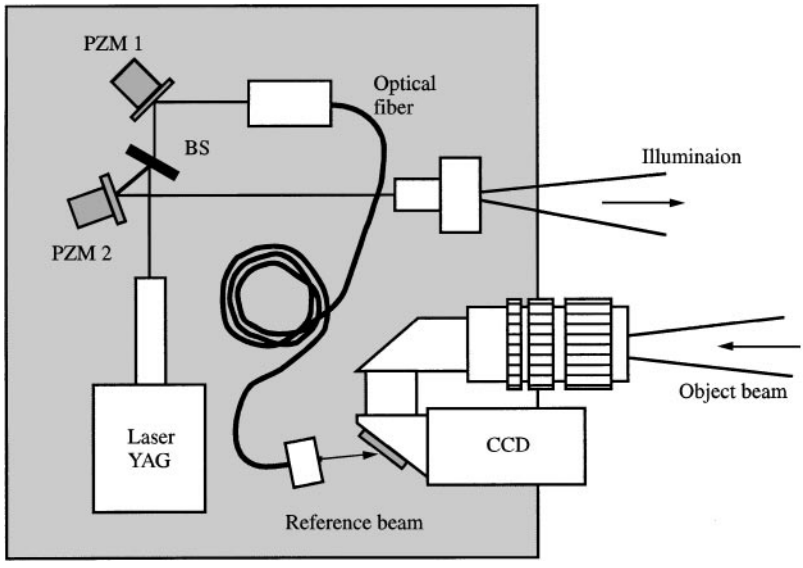

Figure 3. The optical configuration of the TV holography system used for sound field measurements. Beam splitter; BS, a piezoelectric-mounted mirror; PZM1, is used for the phase-shift, and the piezoelectric-mounted mirror; PZM2, is used in phase modulated TV holography to measure small amplitudes ($\sim$2 nm) and phase.

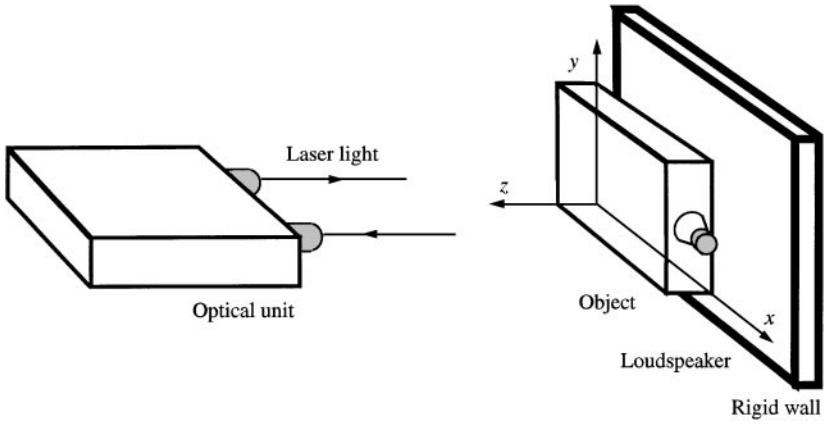

Figure 4. Experimental set-up. The treatment box is placed in front of the optical head. Behind the box a rigid white painted wall is mounted. A loudspeaker is used as an exciter. The laser light travels through the box to the rigid wall and is reflected back again to the optical unit. The box can be tilted to study any projection, in the figure the box is placed for an xy-projection.

proportional to the square of the zeroth-order Bessel function, J_0, as

$$I_{\text{out}}(\mu, \nu) \approx J_0^2\left[\frac{4\pi}{\lambda}\Delta d\right], \tag{8}$$

where (μ, ν) is the pixel co-ordinate on the CCD detector and λ is the wavelength of the laser. The dark fringes occur when equation (8) is equal to zero; this occurs the

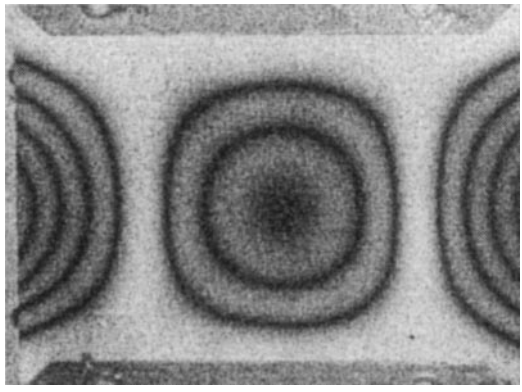

Figure 5. An interferogram of a vibration mode of a rectangular plate clamped along the upper and lower edge. The dark fringes are isolines with equal vibration amplitude. The first dark fringe corresponds to an amplitude of 0·1 μm. The vertical white lines between the antinodes are nodal lines and corresponds to zero amplitude.

first time when the argument $(4\pi/\lambda)(\Delta d) = 2{\cdot}40$. The vibration amplitude must therefore be larger than $\Delta d = 0{\cdot}1$ μm (when using a laser with wavelength 532 nm) to record one or more black fringes. Up to about 20 such fringes may be resolved on the monitor without any difficulties.

Now, assume that instead of a vibrating plate one has a sinusoidally oscillating sound pressure field in the box, as in Figure 4. For simplicity, also assume that the sound pressure is constant along the side $L_z = 0{\cdot}1$ m in the box. An optical path change of $\Delta d = L_z \Delta n = 0{\cdot}1$ μm, that is the first black fringe, corresponds to a sound pressure change which gives a change in refractive index of the air of $\Delta n = 10^{-6}$ for 0·1 m probing depth. Upon using equation (6) this corresponds to a sound pressure level as high as 148 dB. In an attempt to verify this value, a microphone was inserted inside the box. The microphone probe was placed close to the first black fringe, but since the sound field now was slightly changed due to the disturbance of the microphone, it was not possible to measure the sound pressure level exactly at a black fringe. The measured value was slightly lower than the theoretical expected value. It was realized that the measurement of the sound field in a box by using a microphone does not mean exactly the same as the measurement of the sound field without the disturbing microphone.

It is of course possible to detect smaller vibration amplitudes and sound pressures less than that amount which corresponds to the first fringe of the Bessel function. Upon looking at the interferogram on the monitor an amplitude of about 1/4 of the first fringe can be detected using ordinary TV holography. This is due to the fact that the intensity in the interferogram is lowered quite fast in the low-amplitude range. By using electronic evaluation of the decreasing grey level, even smaller amplitudes, say on the order of 1/10 of that of the first black fringe, can be resolved.

4.1. PHASE-MODULATED TV HOLOGRAPHY

A technique to measure very small vibration amplitudes (in the nanometer range) is phase-modulated TV holography [7–10, 17, 18]. In this technique, the phase of the vibration is also detected. The amplitude sensitivity of the TV holography system is increased by a factor of 50; that is, down to amplitudes in the range of $0{\cdot}1/50 = 2$ nm. For the same examples as before, this technique now corresponds to a sound pressure level in the box of about 114 dB.

Løkberg *et al.* [7–10] have used phase-modulated TV holography to measure phase and amplitude of propagation harmonic sound fields. Saldner [18] later presented a combination of phase stepping and the sinusoidal phase-modulation technique.

In the interferograms presented in this paper, ordinary TV holography is used for the sound pressure field measurements. The frequencies of the aerial standing waves are easily detected with this technique. The phase of the sound field is however measured by using the phase-modulated technique as described by Saldner [18]. The phase of the sound field is determined from the expression [17]

$$\theta = \arctan\left[\frac{I_{090} - I_{270}}{I_{180} - I_{000}}\right], \tag{9}$$

where I_{xxx} are four successive recorded images with an increased phase modulation of 90° in between them. However, for vibration amplitudes and sound pressure close to zero, both the nominator and the denominator in equation (9) will be close to zero, and the measured phase will be very uncertain. To reduce the noise, a spatial convolution algorithm is applied, which lowers the spatial resolution at the nodes considerably.

5. RESULTS

A high number of different standing waves are experimentally found in the box by using ordinary TV holography. In Table 1 some of the eigenmodes are listed, showing the measured and the theoretical frequencies of the modes presented in Figures 6–12. Even though the theoretical values are for a box with rigid walls, which the PMMA box does not have, the eigenfrequencies coincide quite well. For low frequencies the deviation is larger, mainly caused by the interaction of the enclosed vibrating air with the vibrating walls [19].

In Figures 6–12 amplitude and phase distribution of some selected modes are shown. The three small black spots, seen in the middle of each interferogram, are due to mirror reflections in the walls of the box. First some examples of "classical" mode shapes, thereafter two examples of coupled modes, are shown.

In Figure 6, the simple (2, 0, 0) mode at 684 Hz is shown. The standing wave has a wavelength equal to the length of the box in the x-direction ($\lambda = 0{\cdot}5$ m). There are two broad nodal lines perpendicular to the x-axis. These fringes are seen in both the xy-plane, Figure 6(a), and the xz-plane, Figure 6(b). The dark fringes (or area) in the centre are in opposite phase relative to the fringes at the walls; compare with Figure 6(c). The sound pressure in Figures 6(a), (b) may seem to differ a bit even if

TABLE 1

Frequencies for some standing waves in a rectangular box of PMMA with a dimension of 0·5, 0·3, 0·1 m; *theoretical values are for a rigid box using the sound speed* 345 m/s; *experimental values are measured by using TV holography*

Mode	Theoretical frequency [Hz]	Measured frequency [Hz]
(2, 0, 0)	690	684
(6, 0, 0)	2070	2067
(5, 2, 0)	2073	2067
(0, 4, 0)	2300	2298
(3, 4, 0)	2522	2521
(8, 0, 0)	2760	2757
(10, 0, 0)	3450	3453
(0, 0, 2)	3450	3453
(2, 0, 2)	3518	3519

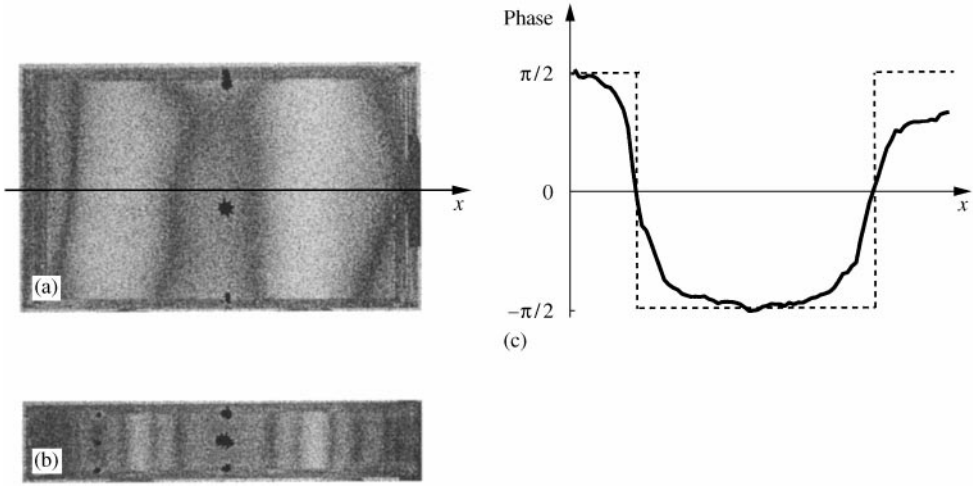

Figure 6. Interferogram showing an aerial standing wave at 684 Hz, mode (2, 0, 0). (a) View through the upright box, *xy*-projection; (b) view through the side of the box, *xz*-projection; (c) the phase along the *x*-axis of the box. Solid line is the measured phase and dotted line is the theoretical expected phase distribution.

the driving voltage is equal. This is due to the fact that the sound pressure field seen in the figures are the integrated sound pressure along the laser illumination direction through the box. Since the box is rectangular the integration distance is five times longer in Figure 6(b) than in Figure 6(a). Therefore, a higher number of dark fringes are seen in Figure 6(b) than in Figure 6(a). In addition, the effect of the slightly divergent illumination direction has a larger influence in Figure 6(b) than in Figure 6(a). Therefore, the most striking result shown in Figure 6(b) is that the sound pressure is constant in the *z*-direction. The sound pressure level is more easily determined from Figure 6(a).

The phases of the standing waves shown in Figures 6(c), 7(c) and 8(c) are evaluated from equation (9). For those points where the amplitude is rather low, both the numerator and the denominator in equation (9) will be close to zero. The phases at those points will be very noisy and hard to evaluate. Applying a convolution smoothing algorithm to the measurement will decrease the noise but due to spatial averaging the step in phase from $\pi/2$ or $-\pi/2$ will not get as steep as expected. Therefore, Figures 6(c), 7(c) and 8(c) have two curves, one solid curve with the actual measured phases and with the spatial averaging applied, and one dotted curve with the theoretical expected values. The value of the phase at the right-hand side of the box in Figure 6(c) is not exactly $\pi/2$ as expected. But notice that this is where the loudspeaker is positioned, so the deviation might be explained by the influence from the loudspeaker.

In Figure 7, the (0, 4, 0) mode at 2298 Hz is shown. Here there is a standing wave pattern seen only in the y direction. The wavelength is half the height of the box ($\lambda = 0{\cdot}15$ m). Note that in this case, dark fringes are seen only in the xy-plane, Figure 7(a), and not in the xz-plane, Figure 7(b). A probing ray through a standing wave will experience equal amounts of high and low sound pressures along the path which in total add up to a zero optical phase change in the y-direction; that is, no fringes are not be expected in the xy-plane. The dark fringes at the upper and lower walls are in phase with the dark fringe in the centre and in phase opposite to the others; see Figure 7(c).

Figure 8 shows a more complicated mode labelled (2, 0, 2) at 3519 Hz. In this mode there are standing waves in two directions. There are nodal lines both in the x and the z directions see Figure 8(b). The sound wave is now travelling around the box and is reflected at the walls at angles not equal to 90° [12]. No fringes are seen

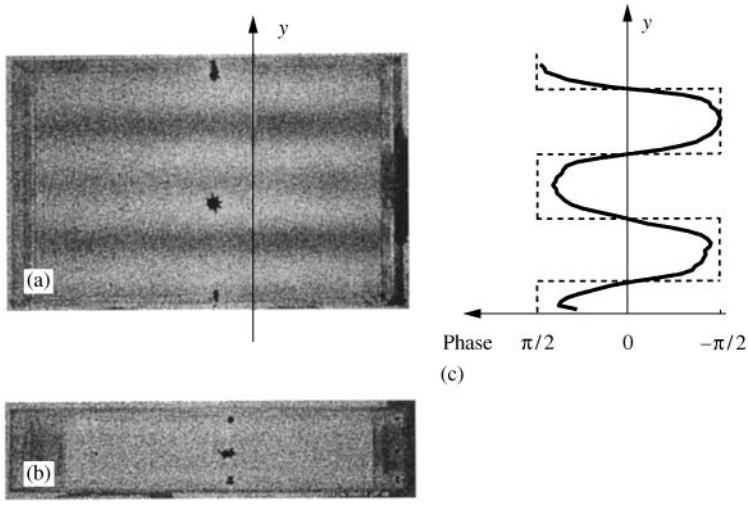

Figure 7. Standing wave at 2298 Hz, mode (0, 4, 0). (a) View through the upright box, xy-projection; (b) view through the side of the box, xz-projection; (c) the phase along the y-axis of the box. Solid line is the measured phase and dotted line is the theoretical expected phase distribution.

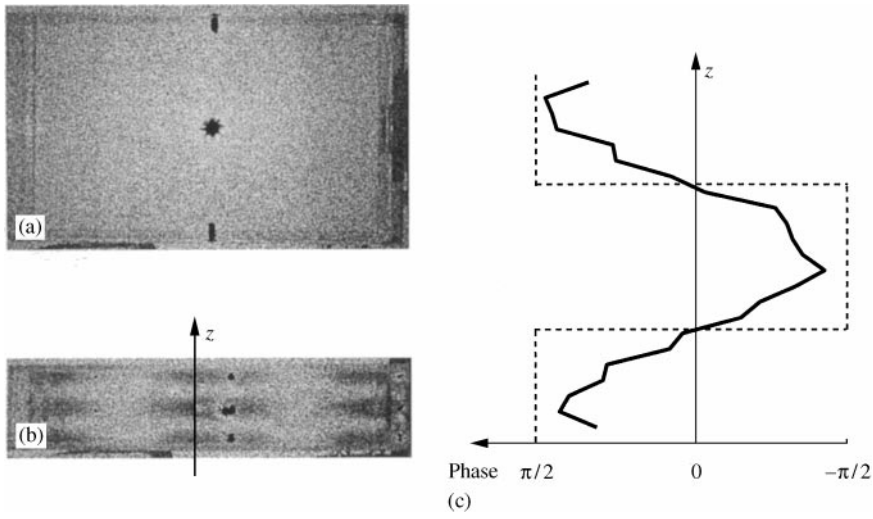

Figure 8. Standing wave 3519 Hz, mode (2, 0, 2). (a) View through the upright box, xy-projection; (b) view through the side of the box, xz-projection; (c) the phase along the z-axis of the box. Solid line is the measured phase and dotted line is the theoretical expected phase distribution.

in the xy-plane; see Figure 8(a), since the probing light ray in the z direction will experience a phase variation as in Figure 8(c) which adds up to a zero optical phase change [cf. with Figure 7(b)]

Figure 9 shows the xy-projection of a very regular mode (8, 0, 0) at 2757 Hz. This mode has a standing wave in the x-direction and the wavelength is one-fourth of the length of the box ($\lambda = 0{\cdot}125$ m)

Figure 10 shows the mode (3, 4, 0) at 2521 Hz. This is the "classical" shape of a two-dimensional mode, as the mode (2, 0, 2) in Figure 8.

In this investigation, modes of "non-classical" shape, such as combination modes [20], were also detected. Two examples of such modes are shown in Figures 11 and 12.

Figure 11(a) shows a combination mode at 3453 Hz. The interferogram in Figure 11(a) differs from those of the "classical" modes; see Figures 6–10. The interference pattern is now staggered. In other two-dimensional modes, for examples mode (3, 4, 0) in Figure 10, the interference fringes are formed in aligned configurations. Theoretically, the two modes (10, 0, 0) and (0, 0, 2) both appear at frequency 3450 Hz. A possible explanation of this odd pattern in Figure 11(a) is that the modes (10, 0, 0) and (0, 0, 2) are excited simultaneously. Studying the phase of the sound pressure of the two modes [see Figure 11(b)] leads to a pattern that corresponds to the pattern found in Figure 11(a).

In Figure 12(a) another strong combination mode is shown. The mode found at 2067 Hz reminds one of the mode (6, 0, 0) but is not "classical" in shape. The nodal lines, for example, are not straight lines. The reason for this spatial distribution might be an influence from mode (5, 2, 0) which is really close in frequency. The theoretical frequency for mode (6, 0, 0) is 2070 Hz and for mode (5, 2, 0) it is

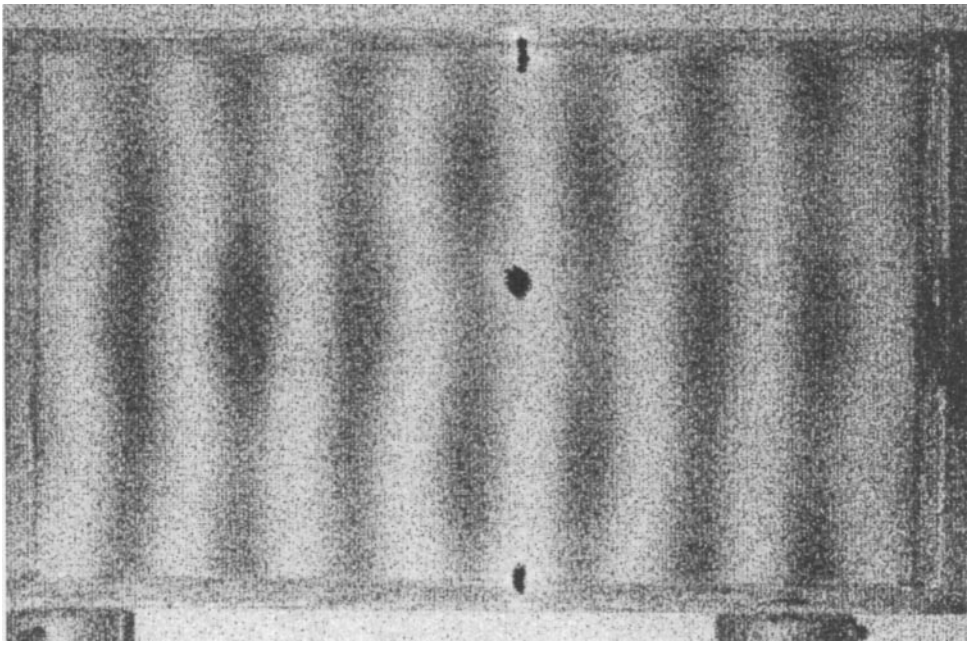

Figure 9. Standing wave at 2757 Hz, mode (8, 0, 0), view through the upright box, the xy-projection.

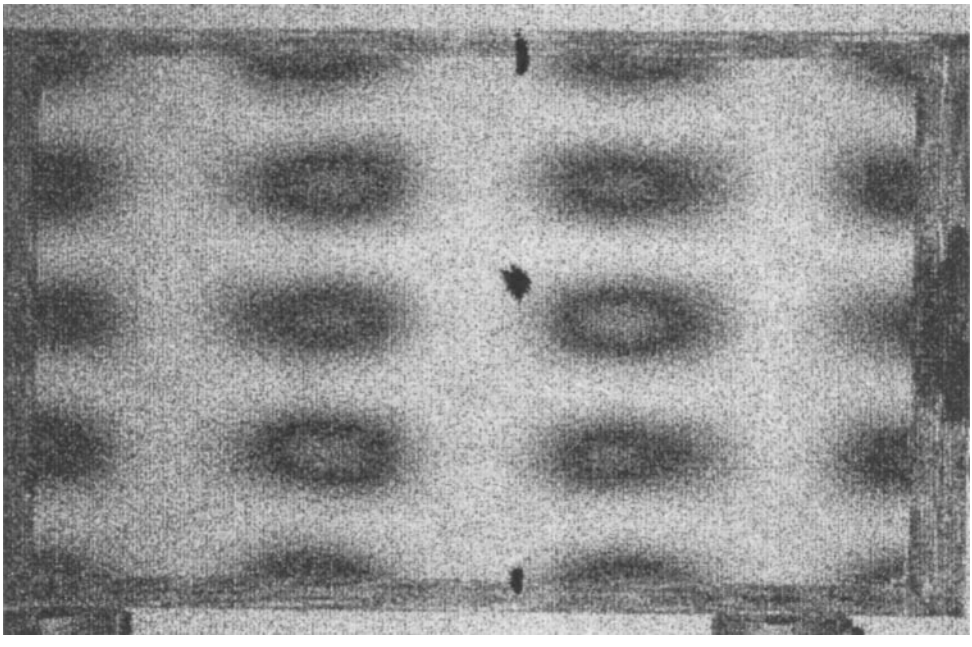

Figure 10. Standing wave at 2521 Hz, mode (3, 4, 0), view through the upright box, the xy-projection.

2073 Hz. Upon studying the phases of these two modes, see Figure 12(b), in the same way as in Figure 11 it is found that this is a reasonable explanation. But it

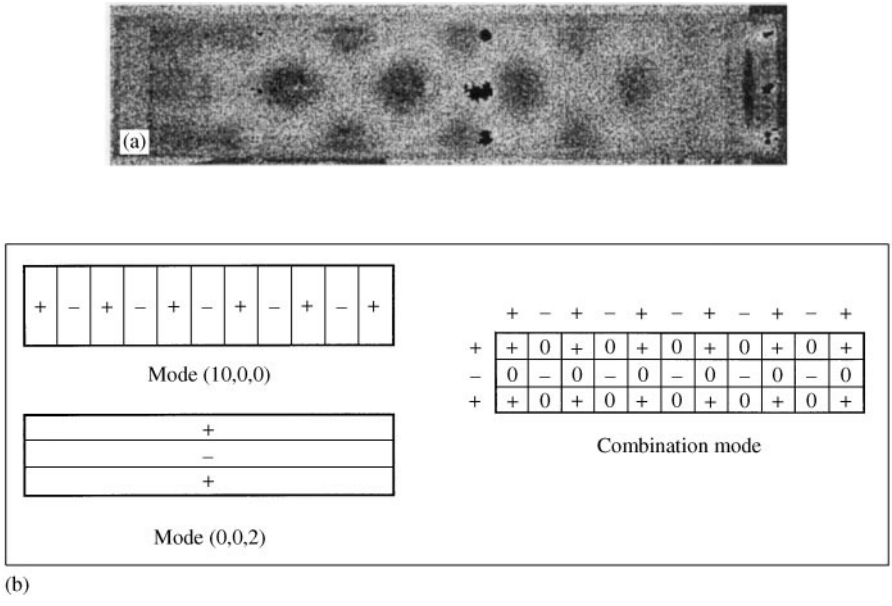

Figure 11. Standing wave at 3453 Hz. (a) View through the side of the box, the *xz*-projection; (b) phase distribution for modes (10, 0, 0) and (0, 0, 2) and the phase of the combination of the two modes. The result coincides with the combination mode found in (a).

cannot be ruled out that the phase distribution of the loudspeaker or the will vibrations also interact in this mode.

With the TV holography equipment used, it is also easy to show the influence of obstacles or changes in the set-up since this is real-time measuring technique.

The interferogram in Figure 13 shows the mode (2, 0, 0) (cf. with Figure 6) when a microphone probe is placed in the sound field inside the box. It is interesting to notice that the microphone disturbs the sound field quite a lot. The interference fringes have lower contrast than in the case without the microphone; cf. with Figure 6(a). This indicates that the sound pressure is slightly lower. The frequency is also changed. With the microphone placed inside the box, the standing wave (2, 0, 0) is found at 692 Hz, which is 8 Hz higher than in the situation without the microphone (684 Hz). It is thus easy to show that the inserted microphone acts as a disturbance in the cavity that changes both the resonance frequency and the amplitude. It has to be realized that placing a microphone in a sound field means that the measuring situation has changed.

How do the standing aerial waves interact with the box? With TV holography it is also possible to measure the structural vibrations of a shell structure. In Figure 14, the structural vibrations of the rectangular box are shown together with the sound pressure field. The upper-half of the box has been painted white to make the wall visible in the laser light, so the structural vibration could be measured. The lower part of the box was left transparent so one was able to measure the sound pressure field inside the box. Since the structural vibration amplitudes for low frequencies often are high, it was not always possible to measure the vibration

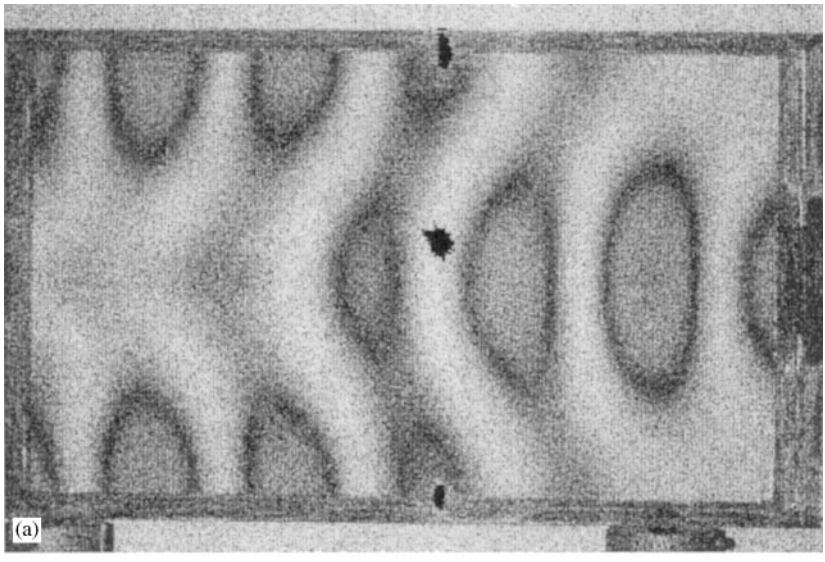

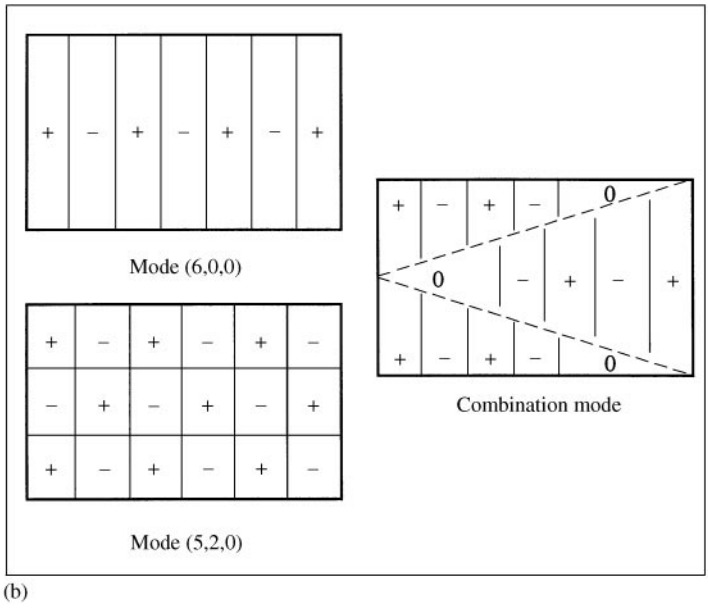

Figure 12. Standing wave at 2067 Hz. (a) View through the upright box, the *xy*-projection; (b) phase distribution for modes (6, 0, 0) and (5, 2, 0) and the phase of the combination of the two modes. The results coincide with the combination mode found in (a).

amplitude of the walls and the sound pressure field simultaneously. The structural vibrations were therefore measured at the same frequencies and the same conditions as the standing waves but at lower sound pressures. In Figure 14(a) mode (2, 0, 0) at 684 Hz is shown; cf. with Figure 6. The structural vibration in the upper-half of Figure 14(a) is found at only 1/100th of the driving voltage of the

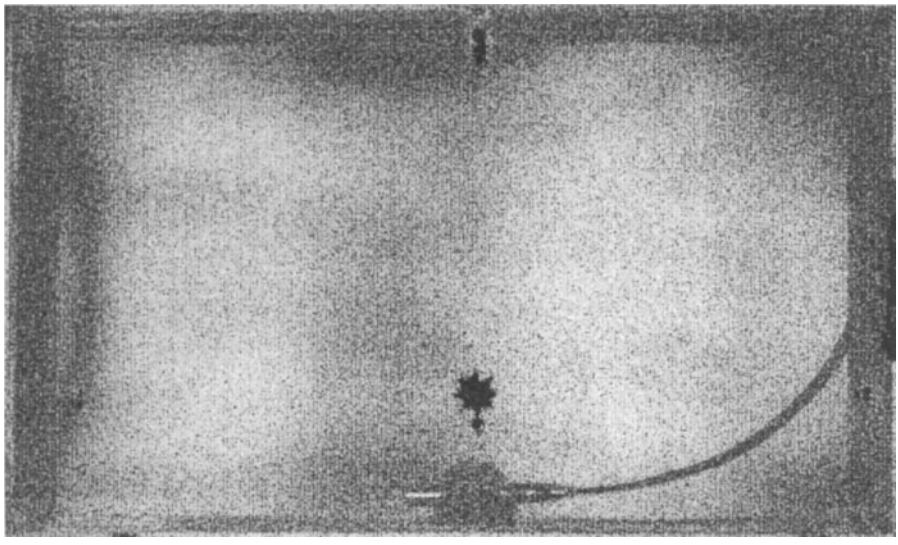

Figure 13. Mode (2, 0, 0), view through the upright box, the xy-projection. A microphone probe is placed in the sound field. The frequency of the standing wave with microphone is changed to 692 Hz; compare the amplitude distribution to that of Figure 6.

loudspeaker for the sound pressure field in the lower-half of the figure. In Figure 14(b) the mode (0, 4, 0) at 2298 Hz is shown; cf. with Figure 7. Here the driving voltage is one-tenth of the one used for the sound field. Notice how the antinodes in the walls are mostly located along the antinodes in the sound pressure field, but that the structural vibrations have a much more complicated shape (operational deflection shape). In Figure 14(a), the vibration pattern of the wall is mainly orientated vertically as is the sound pressure field, and in Figure 14(b) horizontally. A simple shape of the aerial wave pattern inside a cavity does not correspond to a simple vibration pattern of the surrounding walls nor a simple phase distribution.

Standing waves in non-regular enclosures, as in reference [21], are also possible to measure with the same technique as described above. In Figure 15 a standing wave pattern at 996 Hz inside the sound box of a guitar is shown. The guitar is an ordinary modern acoustical guitar with the top and back plates replaced by PMMA plates. The mode is excited by a loudspeaker placed at the sound hole of the guitar, seen in the figure. This mode looks very much the same as the fifth air cavity mode of a guitar at 956 Hz, described by Fletcher and Rossing [22]. That mode is described as having two vertical nodal lines, one on each side of the sound hole. The antinodes at the vertical walls are vibrating in phase and opposite in phase to the central part. At the sound hole a vibrating air column is formed; that is, this mode generates a considerable amount of sound at the sound hole. The mode seen in Figure 15 shows essentially the same standing wave pattern, but the antinodes are quite curved and the centre antinode area consists of two parts vibrating in phase with more or less a saddle point in between them. The exact

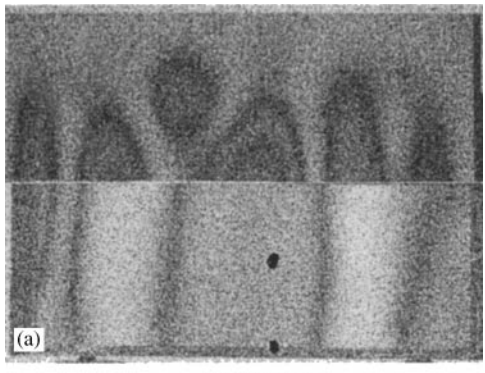

Mode (2,0,0)

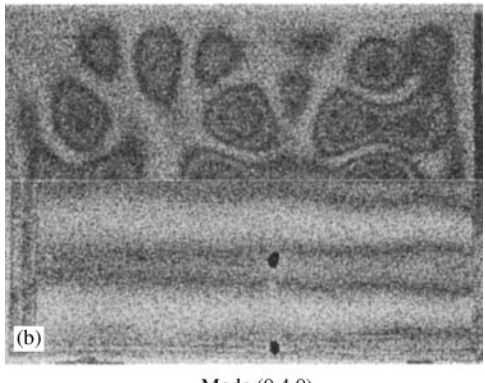

Mode (0,4,0)

Figure 14. Operational deflection shapes (ODSs) of the wall of the rectangular box, upper-half, and internal sound pressure field, lower-half. (a) For mode (2, 0, 0); (b) for mode (0, 4, 0); compare with Figures 6 and 7. The ODSs are excited in the same way as the sound pressure field but at lower sound pressure, about 1/100 in (a) and 1/10 in (b) of the driving voltage of the loudspeaker.

position and shape of the antinodes are easily measured by the TV holography technique.

6. DISCUSSION

Standing-wave patterns in a sound box have been measured by using ordinary TV holography. With this method it is possible to "see" the sound in real time. The frequencies and the shape at the standing waves are easily detected. The pases of the sound fields are also measured. All this can be done in full field and without disturbing the sound field.

With two examples it has been shown that it is possible to investigate the interaction between the enclosed sound field and the structural vibrations. The antinodes in the structural vibration seem in these examples to line up with the aerial ones. The operational deflection shapes in amplitude and phase of the structure are

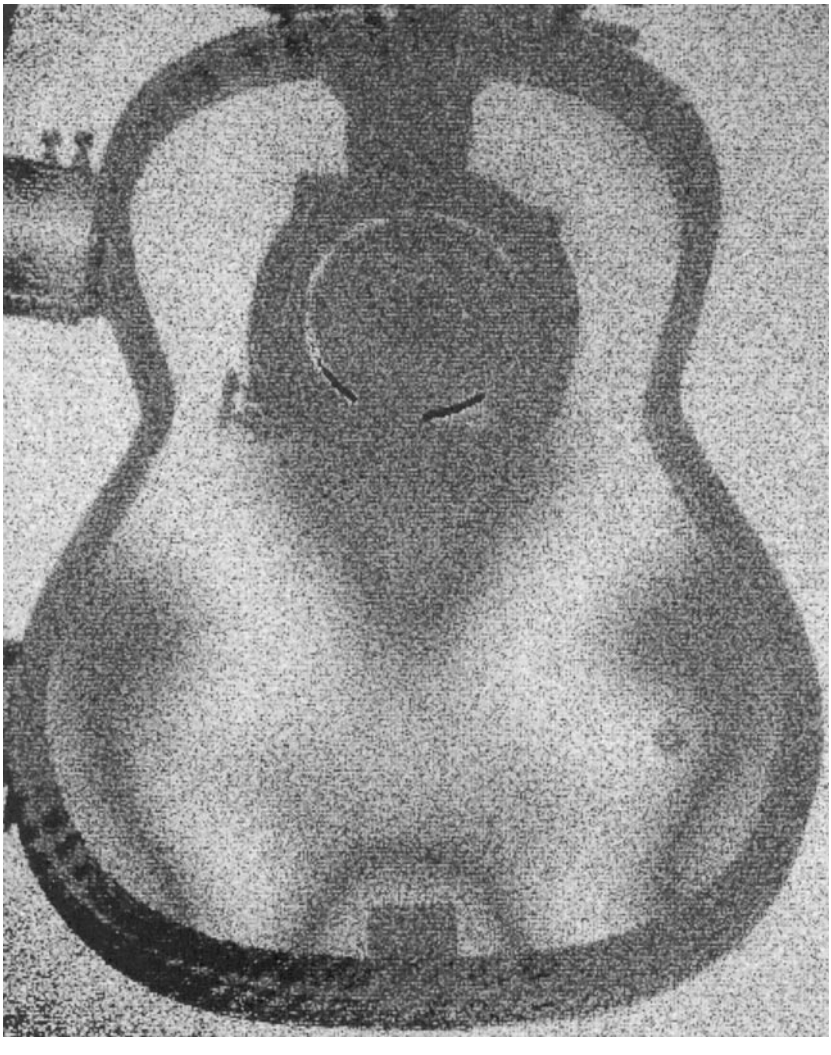

Figure 15. Standing wave inside the sound box of a guitar. The mode is found at 996 Hz in an ordinary guitar with the top and back plates replaced with PMMA plates. A loudspeaker placed outside the sound hole is used as the exciter.

however much more complicated than the standing wave pattern of the sound pressure field.

For the experimental set-up used in this paper the sound pressure needs to be quite high. The index of refraction times the integration distance (the depth of the sound field), that is the change in optical phase, needs to be 0·1 μm to fully detect the first black fringe in the interferogram. This corresponds to a sound pressure level as high as 148 dB for a sound field with depth (integration distance) 0·1 m. For an inegration length 10 times deeper, 1 m, the sound pressure level still needs to be as high as 128 dB. This is however not as bad as it looks at first sight since the sound pressure easily gets very high in the antinodes of a standing wave in an enclosure.

Since the illumination beam travels through the transparent box, in the z-direction in Figure 4, the measured sound field is an xy-projection: that is, a two-dimensional projection of the three dimensional sound field. For a complete three-dimensional reconstruction of the sound field, a tomographic routine needs to be used [9–11] where a number recordings from several directions are obtained.

One error in the experiments reported is that the projection of the sound field is not exactly in the z-direction (see Figure 4), but along the divergent illumination direction. The object, the transparent box, is placed fairly close, about 1·2 m from the optical head and the illumination and the observation directions are not completely parallel. Therefore, the projection is slightly disturbed: i.e., the angle of incidence of the illumination is not 90° throughout the entire box. Only in the centre of the box is there a perfect xy-projection. This problem can however be avoided by placing the object far from the optical head or by using collimated light. This problem gets more severe when looking through the longer side of the box; for instance see Figure 11(a) on the right and left sides.

For a standing wave in the depth of the box, the z-direction in Figure 4, the phase of the sound is alternating between positive and negative values. For an integration through an even number of such alternations the result is zero in optical phase change. It is thus not always possible to detect a standing wave in the depth, even if it is excited. This is the case in Figure 7(b), mode (0, 4, 0), and 8(a), mode (2, 0, 2), where no standing wave is detected from that viewing direction. These modes are detected from other viewing directions of the box; see Figures 7(a) and 8(b). It must be remembered in the interpretation of the figures that they show the integrated projected sound pressure and the phase has to be taken into account.

It is also shown that a microphone placed in the sound field disturbs both the sound pressure field and changes the resonance frequency. Measuring a sound field with a microphone does not necessarily give the same result as without the microphone probe. The non-contacting TV holography technique does not introduce disturbances as the microphone does.

The technique described here can be used to illustrate standing-wave phenomena in non-symmetric boxes: for example, a cabin of a car or a musical instrument as in Figure 15. It is also very useful for the demonstration of standing waves and it might provide useful information for textbooks in acoustics.

ACKNOWLEDGMENTS

The Swedish National Board for Industrial and Technological Development-NUTEK has supported this work. The JC Kempe foundation has financed the upgraded TV holography system.

REFERENCES

1. Lord Rayleigh 1877 *The Theory of Sound*, Vol. II. New York: Dover Publications, second edition, 1945 re-issue, 57–58.
2. Strehlke 1855 *Annalen der Physik und Chemie* **95**, 577–602. Ueber die Schwingungen homogener elastischer Scheiben.

3. F. J. Fahy 1989 *Sound Intensity*. London: E & FN Spon, an imprint of Chapman & Hall, second edition, 1995 re-issue, 89–148.
4. R. L. Powell and K. A. Stetson 1965 *Journal of Optical Society of America* **55**, 1593–1598. Interferometric vibration analysis by wavefront reconstruction.
5. A. O. Wåhlin, P. O. Gren and N.-E. Molin 1994 *The Journal of the Acoustical Society of America* **96**, 2791–2797. On structure-borne sound: experiments showing the initial transient acoustic wave field generated by an impacted plate.
6. S. Schedin, A. O. Wåhlin and P. Gren 1996 *The Journal of the Acoustical Society of America* **99**, 700–705. Transient acoustic near field in air generated by impacted plates.
7. O. J. Løkberg 1994 *Applied Optics* **33**, 2574–2584. Sound in flight: measurement of sound fields by use of TV holography.
8. O. J. Løkberg 1994 *The Journal of the Acoustical Society of America* **96**, 2244–2250. Recording of sound emission and propagation in air using TV holography.
9. O. J. Løkberg, R. Rustad and M. Espeland 1994 *Vibration Measurements* **2358**, 305–312. Reconstruction of sound fields using TV holography.
10. O. J. Løkberg, M. Espeland and H. M. Pedersen 1995 *Applied Optics* **34**, 1640–1645. Tomographic reconstruction of sound fields using TV holography.
11. P. Gren, S. Schedin and X. Li 1998 *Applied Optics* **37**, 834–840. Tomographic reconstruction of transient acoustic fields recorded by pulsed TV holography.
12. L. L. Beranek 1954 *Acoustics*, 285–297. New York: Mcraw-Hill Book Company.
13. A. D. Pierce 1981 *Acoustics—An Introduction to its Physical Principles and Applications*. New York: Acoustical Society of America, second edition, 1989 re-issue, 284–287.
14. C. M. Vest 1979 *Holographic Interferometry*, 344. New York: Wiley.
15. K. A. Stetson, W. R. Brohinsky, J. Wahid and T. Bushman 1989 *Journal of Nondestructive Evaluation* **8**, 69–76. An electro-optic system with real-time arithmetic processing.
16. K. A. Stetson 1990 *Proceedings of the Society for Experimental Mechanics Conference on Hologram Interferometry and Speckle Metrology, Baltimore, Maryland, USA*, 294–300. Theory and application of electronic holography.
17. O. J. Løkberg 1993 *Speckle Metrology* (R. S. Sirohi, editor), 182. New York: Marcel Dekker, Inc. Recent development in video speckle interferometry.
18. H. O. Saldner 1996 *Applied Optics* **35**, 3791–3798. Phase-stepped television holographic technique for measuring phase and amplitude maps of small vibrations.
19. A Isaksson, H. O. Saldner and N.-E. Molin 1995 *Journal of Sound and Vibration* **187**, 451–466. Influence on enclosed air on vibration modes of a shell structure.
20. N.-E. Molin and K. A. Stetson 1969 *Journal of Scientific Instruments* (*Journal of Physics E*) **2**, 609–612. Measuring combination mode vibration patterns by hologram interferometry.
21. E. V. Jansson 1977 *Acustica* **37**, 211–221. Acoustical properties of complex cavities. Prediction and measurement of resonance properties of violin-shaped and guitar-shaped cavities.
22. N. H. Fletcher and T. D. Rossing 1991 *The Physics of Musical Instruments*, 215. New York: Springer-Verlag, Inc.